

Narrow-band-noise generation in charge-density-wave compounds

D. DiCarlo, J. McCarten, T. L. Adelman, M. P. Maher, and R. E. Thorne

Laboratory of Atomic and Solid State Physics and Materials Science Center, Cornell University, Ithaca, New York 14853

(Received 2 December 1993)

The absolute magnitude of the narrow-band noise is estimated within the framework of the Fukuyama-Lee-Rice model. The noise is predicted to vary with sample volume \mathcal{V} as $\mathcal{V}^{-1/2}$, as has been previously noted, and with impurity concentration n_i as $n_i^{1/2}$. Experiments on the sliding charge-density wave in NbSe₃ agree with both of these predictions. The predicted magnitude differs from that observed in NbSe₃, but it is in quantitative agreement with data for the charge-density waves in K_{0.3}MoO₃ and (TaSe₄)₂I. These results provide additional evidence both for bulk narrow-band-noise generation and for weak pinning.

When a charge-density wave (CDW) is current biased above its threshold current, the corresponding voltage has an oscillating component.^{1,2} This striking manifestation of CDW conduction can have an extremely sharp frequency spectrum, and has been dubbed narrow-band noise (NBN). Early experiments showed that the CDW moves one wavelength during each voltage oscillation period, so that the fundamental oscillation frequency is proportional to the CDW current density.³ Controversy has surrounded the mechanism by which the NBN is produced. Noise generation has been attributed to CDW interaction with impurities in the bulk,⁴⁻⁸ and to CDW-normal current conversion at the contacts.⁹⁻¹¹ Measurements by Mozurkewich and co-workers¹²⁻¹⁴ indicated that the noise amplitude varies with sample volume as $\mathcal{V}^{-1/2}$, implying a bulk generation mechanism, while measurements by Ong and co-workers^{10,15} found that the noise amplitude was independent of sample length, implying contact-generated noise. No quantitative comparisons between these experiments and models of noise generation were reported.

The Fukuyama-Lee-Rice (FLR) model¹⁶ has successfully described many properties of the pinned CDW,^{1,17,18} the qualitative form of the dc I - V characteristic,^{6,19} and CDW mode locking in the presence of combined ac and dc fields.¹⁹⁻²¹ Using a mean field approach to the FLR model, Fisher²² calculated the harmonic content of the NBN for small CDW velocities, and showed that the noise persists at high velocities. Numerical simulations by Matsukawa¹⁹ agreed with Fisher's results, and yielded predictions for the bias dependence of the harmonic content which are in qualitative agreement with experiment.

Here we describe a simplified quantitative estimate of the amplitude of the NBN within the FLR model. The predicted dependencies on volume and impurity density are found to be in excellent agreement with measurements on the CDW conductor NbSe₃. The predicted NBN magnitude disagrees quantitatively with data for NbSe₃, but is in good agreement with previous experiments performed on K_{0.3}MoO₃ and (TaSe₄)₂I.^{13,14}

To calculate the NBN amplitude in the FLR model, we consider a current-biased CDW and calculate the volt-

age necessary to keep the CDW current constant, i.e., to keep the average CDW phase advancing uniformly. The CDW-impurity interaction is given as

$$H_{\text{imp}} = v\rho_1 \cos[\phi(\mathbf{x}_i, t) - \phi_{\text{imp}}], \quad (1)$$

where v is the strength of the impurity, ρ_1 is the CDW's modulation amplitude, $\phi(\mathbf{x}_i, t)$ is the CDW phase at the impurity, and ϕ_{imp} is the impurity's preferred phase. For a rigid CDW sliding past a single impurity, the impurity will alternately pull and push the CDW at a frequency proportional to the CDW's velocity. To maintain a constant CDW current, the oscillating impurity force must be matched by an applied oscillating electric field of magnitude

$$\Delta E_{\text{imp}} = \left(\frac{Q}{e\rho_{\text{eff}}\mathcal{V}} \right) v\rho_1, \quad (2)$$

where Q is the CDW wave vector and $e\rho_{\text{eff}}\mathcal{V}$ is the total CDW charge.

In the presence of many impurities, the CDW will deform due to the influence of the impurity forces, and the deformations will fluctuate periodically in time as the CDW slides. Within lengths smaller than the velocity-velocity correlation length, the CDW phase advances rigidly. Since the impurities are randomly located, the preferred phases at the impurities are random, and the impurity forces add incoherently. Taking ξ^D to be the size of a velocity correlated "domain" and n_i the impurity density, the noise amplitude per domain is given by

$$\Delta E_{\text{dom}} = (n_i \xi^D)^{1/2} \Delta E_{\text{imp}}. \quad (3)$$

CDW motions on longer length scales are uncorrelated, so the voltage oscillations from velocity correlated domains will also add incoherently,

$$\begin{aligned} \Delta E_{\text{NBN}} &= \left(\frac{\mathcal{V}}{\xi^D} \right)^{1/2} \Delta E_{\text{dom}} = (n_i \mathcal{V})^{1/2} \Delta E_{\text{imp}} \\ &= \left(\frac{Q}{e\rho_{\text{eff}}} \right) \frac{v\rho_1 n_i^{1/2}}{\mathcal{V}^{1/2}}. \end{aligned} \quad (4)$$

Since the oscillating force from an impurity is incoherent

with the forces from the other impurities, the total NBN amplitude is independent of the velocity-velocity correlation length and the dimensionality of the sliding state. The NBN is bulk generated, the amplitude vanishes in the thermodynamic limit, and the NBN is predicted to be a finite size effect.^{6,12,19,22}

The pinning strength and absolute density of impurities are not easily measured, but they are directly related to the threshold field for CDW depinning. For weakly pinned CDW's, the three-dimensional (3D) threshold field is given by^{16,18,23}

$$E_T(3D) = \frac{1}{1000} \left(\frac{Q}{e\rho_{\text{eff}}} \right) \left(\frac{\xi_z^2}{\xi_x \xi_y} \right)^2 \frac{(v\rho_1)^4 n_i^2}{f^3}, \quad (5)$$

where ξ_x , ξ_y , and ξ_z are the anisotropic amplitude coherence lengths and f is the CDW elastic constant. Combining this expression with Eq. (4) to eliminate $v\rho_1$ yields

$$\begin{aligned} \Delta E_{\text{NBN}} &= \left(\frac{Qf}{e\rho_{\text{eff}}} \right)^{3/4} (1000)^{1/4} \left(\frac{\xi_x \xi_y}{\xi_z^2} \right)^{1/2} \\ &\times \frac{E_T(3D)^{1/4}}{\nu^{1/2}} \\ &= A \frac{E_T(3D)^{1/4}}{\nu^{1/2}}, \end{aligned} \quad (6)$$

where the constant A depends only upon intrinsic CDW parameters.

To test the predictions of Eq. (6), experiments were performed on undoped and Ta-doped NbSe₃. NbSe₃ was chosen because its NBN spectrum is highly coherent and because impurity pinning in undoped and Ta-doped NbSe₃ has been well characterized and found to be weak.^{17,18,24} NbSe₃ crystallizes into long ribbonlike whiskers, and exhibits two independent CDW's which form below temperatures $T_{P_1} = 145$ K and $T_{P_2} = 59$ K. Undoped and Ta-doped samples with cross-sectional areas between ~ 0.1 and $\sim 100 \mu\text{m}^2$ were mounted onto an alumina substrate. Silver paint contacts were made in a four-probe configuration with a fixed inner contact separation of 0.75 ± 0.05 mm. Samples were cooled using a closed cycle helium refrigerator, and their NBN measured using a two-probe configuration at 125 K and 48 K, temperatures which yield optimum noise quality for the T_{P_1} and T_{P_2} CDW, respectively. The NBN was amplified by a 50 MHz Trontek amplifier and fed into a HP7550 spectrum analyzer. NBN spectra were taken using spectrum analyzer bandwidths of 100 and 300 KHz at CDW velocities corresponding to fundamental NBN frequencies of $\nu_{\text{CDW}} = 20$ and 40 MHz. The NBN amplitude was determined by integrating the power under the NBN peak and averaging over several spectra. Threshold fields were measured in a four-probe configuration. For samples from a given growth, the bulk (3D) threshold was obtained by averaging over values obtained from thick samples.¹⁸ Doping levels within a growth were characterized using the residual resistance ratio, $\text{RRR} = R(300 \text{ K})/R(4 \text{ K}) \propto n_i^{-1}$,^{17,18} which ranged from 30 to 325.

The measured NBN amplitude is affected by the finite amplifier input impedance and by shunting from the

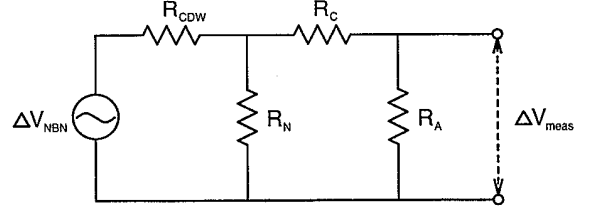


FIG. 1. ac equivalent circuit for the NBN measurements. The intrinsic NBN voltage is shunted by both the normal carriers (R_N) and the amplifier input impedance (R_A). The contact resistance (R_C) and the effective CDW resistance (R_{CDW}) are related to the four-probe and two-probe resistances by $R_4 = R_{\text{CDW}} \parallel R_N$ and $R_2 = R_4 + R_C$, respectively.

large single-particle conductivity in NbSe₃.²⁵ These contributions were modeled using the ac equivalent circuit in Fig. 1. The intrinsic NBN amplitude is related to the measured amplitude by

$$\Delta V_{\text{NBN}} = \frac{1 + R_2/R_A}{1 - R_4/R_N} \Delta V_{\text{meas}}, \quad (7)$$

where R_A is the amplifier's input impedance, R_N is the sample's low-field (normal) four-probe resistance, and R_2 and R_4 are the sample's two-probe and four-probe differential resistances at the CDW current at which the noise measurements are made.²⁶ The oscillating electric field is found by dividing the intrinsic voltage by the contact separation.

Figure 2 shows the sample volume dependence of the NBN amplitude of the T_{P_1} CDW for growths with two different doping levels. Similar results were obtained for a third doping level, and for all doping levels on the T_{P_2} CDW. Fits of each data set to the relation $\Delta E_{\text{NBN}} = B\nu^\alpha$ yield exponents ranging from -0.4 to -0.5 ,²⁷ in very good agreement with the predicted exponent for bulk generated NBN [Eq. (6)] of -0.5 . This

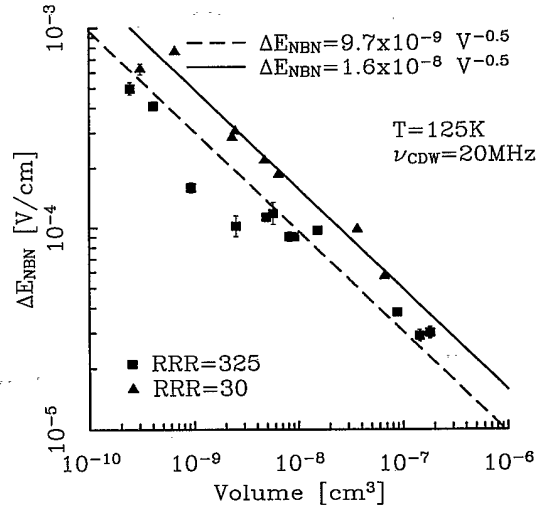


FIG. 2. Volume dependence of the NBN amplitude for the T_{P_1} CDW in undoped ($\text{RRR} = 300$) and heavily doped ($\text{RRR} = 25$) samples.

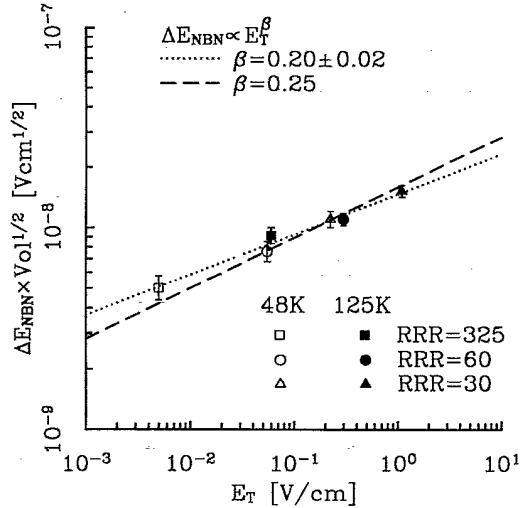


FIG. 3. The amplitude of the NBN determined from fits to the data of Fig. 2 versus threshold field, E_T . The dotted line is the best power law fit to the data for both CDW transitions, and the dashed line is the best fit to the power law expected in weak pinning.

is consistent with the results of Mozurkewich and co-workers.^{12-14,28}

To compare the NBN amplitudes for different doping levels, the data for each temperature and doping level were fit using a power-law exponent of -0.5 and the constant B determined. Figure 3 plots $B = \Delta E_{\text{NBN}} \nu^{1/2}$ versus the bulk threshold field at each doping level, for both CDW's in NbSe₃. For each CDW, the amplitude increases with increasing doping. For each doping level, the amplitude is larger for the high temperature CDW. Fits to the relation $\Delta E_{\text{NBN}} \propto E_T^\beta$ yield exponents of $\beta = 0.18 \pm 0.04$ for the T_{P_1} CDW, $\beta = 0.21 \pm 0.02$ for the T_{P_2} CDW, and $\beta = 0.20 \pm 0.02$ for both CDW's. These exponents are in good agreement with the predicted exponent in Eq. (6) of $\beta = 0.25$. In strong pinning, an exponent of $\beta = 0.5$ is expected.²⁹ In contact-generation models, no impurity concentration dependence of the NBN amplitude is expected. Thus the data in Fig. 3 provide additional evidence both for bulk NBN generation and for weak pinning.

Quantitative comparisons between the predicted and

observed NBN amplitudes can also be made. Using $\xi_x^2/\xi_x\xi_y = 50$,^{30,31} $f = 1.7 \times 10^{-2} \text{ eV \AA}^{-1}$,³² and a CDW condensate density of $\rho_{\text{eff}} = 1.9 \times 10^{21} \text{ cm}^{-3}$ yields a predicted rms amplitude of $\Delta E_{\text{NBN}}(\text{theor.}) \approx 1.6 \times 10^{-6} (\text{V cm})^{3/4} E_T^{1/4} \nu^{-1/2}$ for NbSe₃. The measured rms amplitude is $\Delta E_{\text{NBN}}(\text{expt.}) \approx 1.6 \times 10^{-8} (\text{V cm})^{3/4} E_T^{1/4} \nu^{-1/2}$. The amplitude difference is greater than that expected due to uncertainties in the intrinsic parameters.³³

The predicted $\nu^{-1/2}$ dependence was observed in previous measurements on K_{0.3}MoO₃ and (TaSe₄)₂I.^{13,14} The elastic constants of these materials are not known, but can be estimated from mean field theory using $Qf/e\rho_{\text{eff}} = \hbar v_F/2e$.²³ For K_{0.3}MoO₃, using $\xi_x^2/\xi_x\xi_y \approx 21$,³⁴ $v_F \approx 1.6 \times 10^8 \text{ cm/s}$,³⁵ and $E_T \sim 0.1 \text{ V/cm}$ (Ref. 14) yields a predicted rms amplitude of $\Delta E_{\text{NBN}}(\text{theor.}) \approx 1.8 \times 10^{-6} (\text{V cm}^{1/2}) \nu^{-1/2}$. The measured rms amplitude^{14,36,37} is $\Delta E_{\text{NBN}}(\text{expt.}) \approx 1.7 \times 10^{-6} (\text{V cm}^{1/2}) \nu^{-1/2}$.

For (TaSe₄)₂I, using $\xi_x^2/\xi_x\xi_y \approx 40$,³⁸ $v_F \approx 6 \times 10^7 \text{ cm/s}$,³⁵ and $E_T \sim 2 \text{ V/cm}$ (Refs. 39, 40) yields a predicted rms amplitude of $\Delta E_{\text{NBN}}(\text{theor.}) \approx 1.3 \times 10^{-6} (\text{V cm}^{1/2}) \nu^{-1/2}$. The measured rms amplitude^{13,41} is $\Delta E_{\text{NBN}}(\text{expt.}) \approx 5 \times 10^{-7} (\text{V cm}^{1/2}) \nu^{-1/2}$.

The agreement between the measured and predicted NBN amplitude is remarkably good for K_{0.3}MoO₃ and (TaSe₄)₂I, and much better than for NbSe₃. However, the uncertainties in the predicted values of the former are larger. The origin of the discrepancy in NbSe₃ is unclear, but may be related to additional screening by normal carriers on ungapped portions of NbSe₃'s Fermi surface, which are not present in K_{0.3}MoO₃ and (TaSe₄)₂I.

In conclusion, we have presented experimental data and quantitative analysis for NBN in NbSe₃. We find that the NBN amplitude scales as $\nu^{-1/2}$ and as $E_T^{1/4}$. These results provide additional evidence both for bulk narrow-band-noise generation and for weak pinning.

We wish to thank M. Kvale, S. Ramakrishna, and C. Myers for useful discussions. This work was supported by the NSF (Grant No. DMR-92-04169), and by the MRL program of the NSF (Grant No. DMR-91-21654). R.E.T. acknowledges additional support provided by the Alfred P. Sloan Foundation and by the NSF (Grant No. DMR-89-58515).

¹ For comprehensive reviews of CDW's, see *Electronic Properties of Quasi-One-Dimensional Materials*, edited by P. Monceau (Reidel, Dordrecht, 1985), Part II, p. 139; G. Grüner, *Rev. Mod. Phys.* **60**, 1129 (1988).

² R. M. Fleming and C. C. Grimes, *Phys. Rev. Lett.* **42**, 1423 (1979).

³ P. Monceau, J. Richard, and M. Renard, *Phys. Rev. Lett.* **45**, 43 (1980).

⁴ G. Grüner, A. Zawadowski, and P. Chaikin, *Phys. Rev. Lett.* **46**, 511 (1981).

⁵ P. Monceau, J. Richard, and M. Renard, *Phys. Rev. B* **25**, 931 (1982).

⁶ L. Sneddon, M. C. Cross, and D. S. Fisher, *Phys. Rev. Lett.* **49**, 292 (1982); D. S. Fisher, *ibid.* **50**, 1486 (1983).

⁷ S. E. Barnes and A. Zawadowski, *Phys. Rev. Lett.* **51**, 1003 (1983).

⁸ J. Bardeen, *Phys. Rev. Lett.* **42**, 1498 (1979); **45**, 1978 (1980).

⁹ L. P. Gor'kov, *Pis'ma Zh. Eksp. Teor. Fiz.* **86**, 1818 (1984) [*JETP Lett.* **38**, 87 (1984)].

- ¹⁰ N. P. Ong, G. Verma, and K. Maki, Phys. Rev. Lett. **52**, 663 (1984).
- ¹¹ N. P. Ong and K. Maki, Phys. Rev. B **32**, 6582 (1985).
- ¹² G. Mozurkewich and G. Grüner, Phys. Rev. Lett. **51**, 2206 (1983).
- ¹³ G. Mozurkewich, M. Maki, and G. Grüner, Solid State Commun. **48**, 453 (1983).
- ¹⁴ G. L. Link and G. Mozurkewich, Phys. Rev. B **41**, 11858 (1990).
- ¹⁵ T. W. Jing and N. P. Ong, Phys. Rev. B **33**, 5841 (1986).
- ¹⁶ H. Fukuyama and P. A. Lee, Phys. Rev. B **17**, 535 (1978); P. A. Lee and T. M. Rice, *ibid.* **19**, 3970 (1979).
- ¹⁷ J. W. Brill, N. P. Ong, J. C. Eckert, J. W. Savage, S. K. Khanna, and R. B. Somoano, Phys. Rev. B **23**, 1517 (1981).
- ¹⁸ J. McCarten, D. A. DiCarlo, M. P. Maher, T. L. Adelman, and R. E. Thorne, Phys. Rev. B **46**, 4456 (1992).
- ¹⁹ H. Matsukawa, Synth. Metals **29**, 343 (1989).
- ²⁰ A. A. Middleton, O. Biham, P. B. Littlewood, P. Sibani, Phys. Rev. Lett. **68**, 1586 (1992).
- ²¹ J. McCarten, D. A. DiCarlo, and R. E. Thorne, Phys. Rev. B **49**, 10113 (1994).
- ²² D. S. Fisher, Phys. Rev. B **31**, 1396 (1985).
- ²³ H. Matsukawa and H. Takayama, J. Phys. Soc. Jpn. **56**, 1507 (1987).
- ²⁴ R. E. Thorne, Phys. Rev. B **45**, 5804 (1992).
- ²⁵ Single-particle shunting by R_N is particularly important in comparing the upper and lower CDW's in NbSe₃. While the measured NBN voltage on the lower transition is greater than that on the upper transition, shunting is much greater on the upper transition, so the intrinsic NBN voltage is greater on the upper transition.
- ²⁶ This expression is valid when the applied voltage above threshold $V - V_T$ is much greater than the NBN voltage, which is true except for very close to threshold.
- ²⁷ Data taken at 40 MHz yielded exponents and amplitudes identical to those of the 20 MHz data.
- ²⁸ Detailed predictions for the dependence of the noise amplitude on cross-sectional areas in contact-generation models have not been reported.
- ²⁹ The exponent of $\beta = 0.5$ is obtained by substituting $E_T \propto n_i$ (as assumed in some models of strong pinning) in Eq. (4).
- ³⁰ A. H. Moudden, J. D. Axe, P. Monceau, and F. Levy, Phys. Rev. Lett. **65**, 223 (1990).
- ³¹ D. DiCarlo, E. Sweetland, M. Sutton, J. D. Brock, and R. E. Thorne (unpublished).
- ³² D. DiCarlo, E. Sweetland, M. Sutton, J. D. Brock, and R. E. Thorne, Phys. Rev. Lett. **70**, 845 (1993).
- ³³ The uncertainty in the theoretical NBN amplitude is roughly an order of magnitude.
- ³⁴ S. M. DeLand, G. Mozurkewich, and L. D. Chapman, Phys. Rev. Lett. **66**, 2026 (1991).
- ³⁵ In the tight binding approximation the Fermi velocity is related to the bandwidth D , lattice spacing a_0 , and wave vector Q as $\hbar v_F \approx (Da_0/2)\sin(Qa_0)$. For K_{0.3}MoO₃, an estimated bandwidth of 4 eV (Ref. 1) results in $\hbar v_F \approx 1.1 \times 10^{-7}$ eV cm. For (TaSe₄)₂I, an estimated bandwidth of 2 eV (Ref. 1) results in $\hbar v_F \approx 4 \times 10^{-8}$ eV cm.
- ³⁶ At the temperatures where the NBN was measured in K_{0.3}MoO₃, $\sigma(\text{CDW})/\sigma(N) \gg 10$ (Ref. 37), so shunting by normal carriers is unimportant.
- ³⁷ G. Mihály, P. Beauchêne, J. Marcus, J. Dumas, and C. Schlenker, Phys. Rev. B **37**, 1047 (1988).
- ³⁸ The anisotropy of (TaSe₄)₂I has not been measured, so a value comparable to the anisotropies of NbSe₃ and K_{0.3}MoO₃ is assumed.
- ³⁹ M. Maki, M. Kaiser, A. Zettl, and G. Grüner, Solid State Commun. **46**, 497 (1983).
- ⁴⁰ Z. Z. Wang, M.C. Saint-Lager, P. Monceau, M. Renard, P. Gressier, A. Meerschaut, L. Guemas, and J. Roxuel, Solid State Commun. **46**, 325 (1983).
- ⁴¹ The ΔJ vs \mathcal{V} data for (TaSe₄)₂I in Ref. 13 were converted to ΔE vs \mathcal{V} using resistivity values and I - V curves from Refs. 39 and 40.